

Direct synthesis of methane from CO₂-H₂O co-electrolysis in tubular solid oxide electrolysis cells

Long Chen,^a Fanglin Chen^b and Changrong Xia*^a

^a *CAS Key Laboratory of Materials for Energy Conversion, Department of Materials Science and Engineering & Collaborative Innovation Center of Suzhou Nano Science and Technology, University of Science and Technology of China, Hefei, Anhui 230026, China.*

^b *Department of Mechanical Engineering, University of South Carolina, Columbia, SC 29208, USA.*

* *Fax: +86-551-63601696; Tel: +86-551-63607475; E-mail: xiacr@ustc.edu.cn*

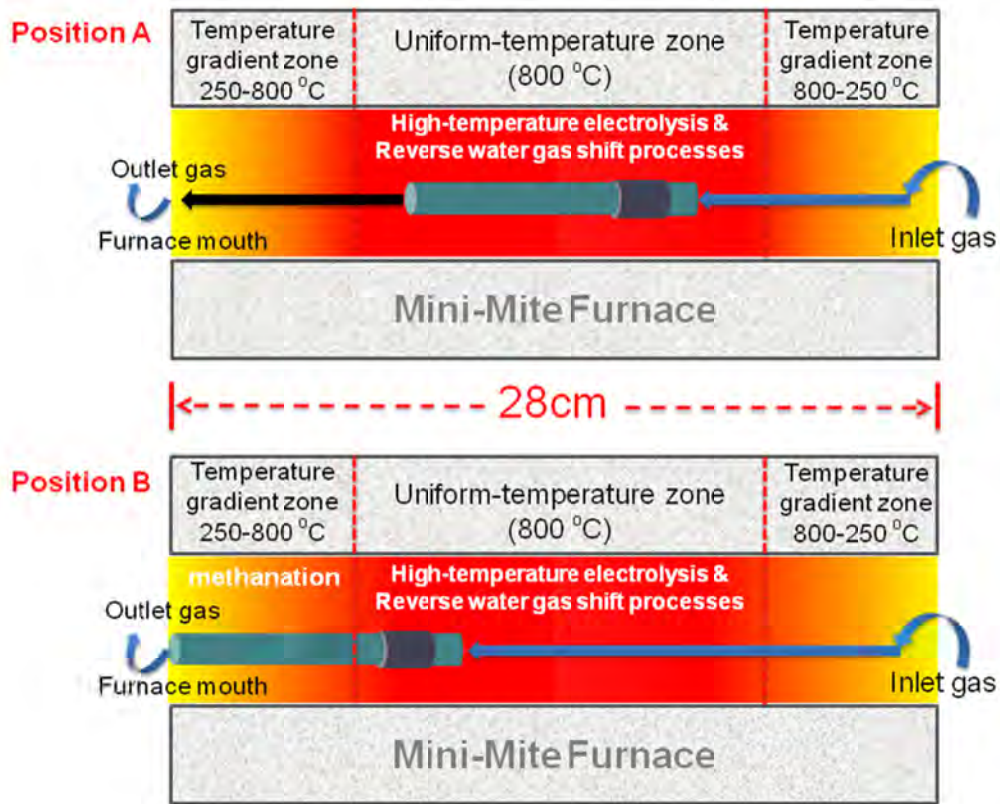


Fig. S1. Schematic showing the temperature distribution of the tubular unit located in a mini-mite furnace (scaled only in the horizontal direction).

Fabrication of tubular unit



Fig. S2 Schematic diagram for the fabrication process of the tubular unit.

The modified phase inversion method¹ can be described as follows. NiO (Jinchuan Group, China) and YSZ (Sichuan, China) powders (weight ratio 1:1) were ball-milled for 24h and used as the raw tube substrate materials. NiO-YSZ was then mixed with polymer solution, which was made from 1-Methyl-2-pyrrolidone solvent (NMP, Chemical Pure, Sinopharm Chemical Reagent Co., Ltd, China, molecular weight : 99.13), polyethersulfone polymer (PESf, Veradel®, Solvay Specialty Polymers, L.L.C., molecular weight : ~63000) and polyvinylpyrrolidone dispersant (PVP, K30, Chemical Pure, Sinopharm Chemical Reagent Co., Ltd, China, molecular weight : ~40000) with weight ratio of NMP : PESf : PVP= 20 : 4 : 1, by ball-milling for 24 h to get a well-dispersed slurry. Another slurry containing 30 wt.% graphite was also prepared. A tube mould (diameter = 0.5 cm) was dip-coated with the graphite slurry and subsequently immersed into tap water for 5 min. After drying, the

tube was coated with NiO-YSZ slurry, and then immersed into ethanol for 10 s, de-moulded, and immersed into tap water for 12 h to complete the phase inversion process (step 1). The dried raw tubes were pre-fired at 1200 °C for 2 h to burn off the graphite and organic components to achieve some structural strength (step 2).

Thin YSZ (TZ-8Y Tosoh) layer was fabricated on the outer surface of the NiO-YSZ tubes by a dip-coating process, and subsequently co-sintered at 1400 °C for 5h (step 3).

A-site non-stoichiometric $(La_{0.85}Sr_{0.15})_{0.9}MnO_{3-\delta}$ (LSM) powder was synthesized using a glycine-nitrate process with La_2O_3 , $Mn(CH_3COO)_2 \cdot 4H_2O$, $Sr(NO_3)_2$ and glycine as the starting materials. La_2O_3 was first dissolved in concentrated nitric acid, and then stoichiometric amounts of $Mn(CH_3COO)_2 \cdot 4H_2O$, and $Sr(NO_3)_2$ were added to form a clear nitrate salt solution, to which glycine was added at a glycine to nitrate molar ratio of 1 : 1. The mixed nitrate-glycine solution was heated on a hot plate until self-combustion took place, yielding very loose black LSM powder. The as-synthesized LSM powder was subsequently calcined at 900 °C for 3 h to remove possible organic residues and to form the perovskite structure. LSM-YSZ composite paste with 40 wt.% YSZ was painted on the electrolyte surface, dried and heated at 1200 °C for 2h. Aqueous solution of $Ce_{0.8}Sm_{0.2}O_{1.9}$ (1.0 M) was impregnated into the LSM-YSZ electrode and fired at 600 °C for 30 min to minimize the electrode polarization resistance. The tubular unites were about 8 cm long with 0.42 cm outer diameter and 0.35 cm inner diameter, and the LSM-YSZ electrode area was about 0.8 cm^2 .

Characterization

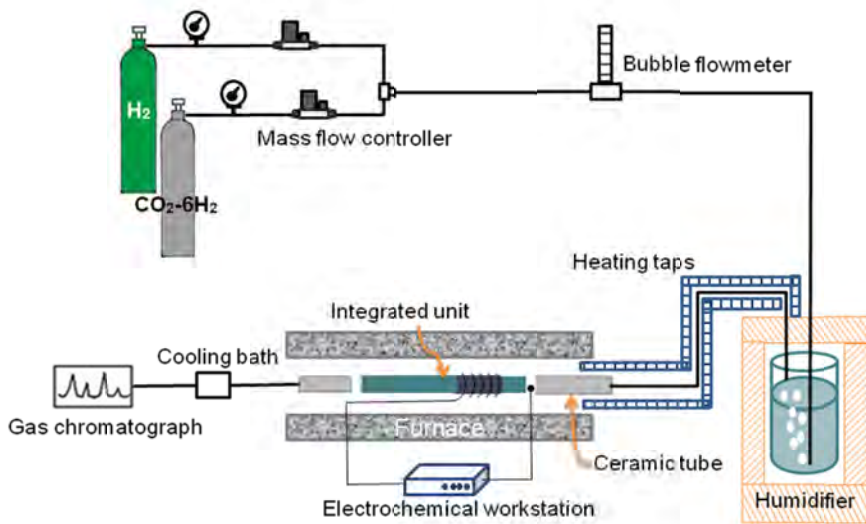


Fig. S3 The schematic of experimental setup for electrochemical tests.

The tubular units were placed in a tube furnace for electrochemical and methanation tests using ambient air at the LSM-YSZ side. Humidity of the inlet gas was controlled using a bubble bottle by assuming 100% relative humidity at every temperature. Heating taps were wrapped around the inlet gas line in order to prevent water condensation during the SOEC operation. The outlet gas was condensed using a cooling bath and then analyzed using an online gas chromatograph (GC9790II, Fuli, Zhejiang, China). The data was obtained after the unit was operated for more than 20 min for various model tests. The porosity of the Ni-YSZ fuel electrode was measured using the Archimedes method. The microstructures of the cells were characterized by scanning electron microscopy (SEM, JSM-6700F). The electrochemical performance of the tubular unit was measured using an electrochemical workstation (Solartron

1287A-1260A). The electrochemical impedance spectra (EIS) were measured under open-circuit conditions in the frequency range from 1 MHz to 0.01 Hz. The amount of hydrogen produced from the SOEC process is calculated by the Faraday's law, assuming 100% current efficiency.²

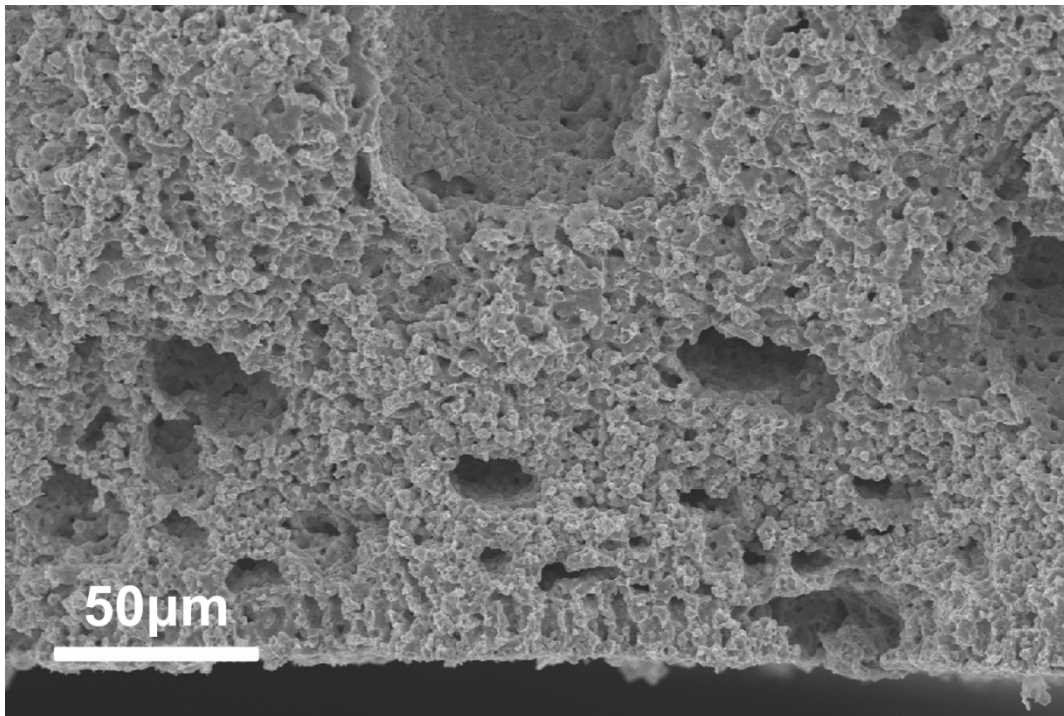


Fig. S4 SEM picture for Ni-YSZ of the inner side of the tubular structure.

Fig. S4 reveals the magnified cross-sectional microstructure near the inner surface of the post-tested Ni-YSZ tubular substrate. There are many small finger-like pores in the skin layer area, and these finger-like pores cross the inner surface and the skin layer and thereby connect these two areas. Apparently, the high porosity of the Ni-YSZ substrate is beneficial for gas transport.

Table S1 Operating conditions and test results for CH₄ production.

Model No.	Operating conditions (800 °C, 20vol.% H ₂ O)	Inlet gas CO ₂ -H ₂ (1:6, volume ratio), Gas flux (mL min ⁻¹)		Gas product composition (%) ± standard error			Total CO ₂ Conversion ratio(%)	CH ₄ yield ratio(%)
		Inlet CO ₂	Outlet CO ₂ +CO+CH ₄	H ₂	CO ₂	CO		
I	Position A (see Fig. S1), Reverse water gas shift (RWGS)	2.16	2.13	69.69±0.02	14.33±0.17	15.98±0.15	0	52.7
	Position A, RWGS & SOEC	1.3V 1.5V	2.14 2.16	74.11±0.25	8.65±0.14	17.24±0.11	0	66.6
II	Position B (see Fig. S1), RWGS & methanation	2.15	2.13	75.72±0.09	5.97±0.18	18.31±0.10	0	75.4
	Position B, RWGS & methanation & SOEC (1.3V)	2.14	2.11	70.66±0.36	14.33±0.36	9.99±0.30	0.09	51.2
III	Position B, RWGS & methanation	2.14	2.11	71.13±0.21	10.58±0.19	6.46±0.01	11.84±0.07	63.4
	24 h short-term test							
IV	1.3V, 1h	2.14	2.11	71.13	10.58	6.46	11.84	63.4
	1.3V, 2h	2.16	2.12	71.80	10.11	6.42	11.67	64.2
IV	1.3V, 3h	2.14	2.14	70.96	10.43	6.55	12.06	64.1
	1.3V, 6h	2.15	2.10	71.75	10.24	6.85	11.17	63.8
IV	1.3V, 9h	2.16	2.10	71.43	10.48	6.70	11.20	63.3
	1.3V, 16h	2.13	2.11	72.08	10.05	6.82	11.06	64.0
IV	1.3V, 18h	2.17	2.15	71.23	10.03	7.21	11.53	65.2
	1.3V, 21h	2.15	2.11	70.53	10.18	7.88	11.41	65.5
IV	1.3V, 24h	2.16	2.14	70.61	10.60	8.11	10.68	63.9
								36.3

Here, total CO₂ Conversion ratio(%) = { [CO]₊ [CH₄] } /{[CO₂] + [CH₄] } ; CH₄ yield ratio(%) = [CH₄] /{[CO₂] + [CO]₊ [CH₄] }. All the concentrations are from the outlet gas.

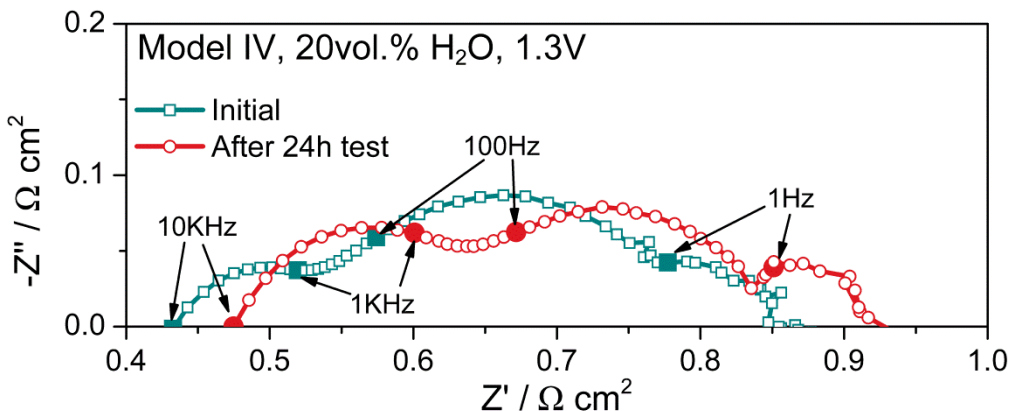


Fig.S5 Impedance spectra for the cell measured before and after 24h short term test under the electrolysis conditions

Fig. S5 shows the impedance spectra for the cell part of the tubular unit measured before and after 24h short-term test. The ohmic resistance slightly increased from 0.44 to 0.48 $\Omega \text{ cm}^2$, while the cell polarization resistance is essentially unchanged. Overall, the cell electrochemical performance is relatively stable.

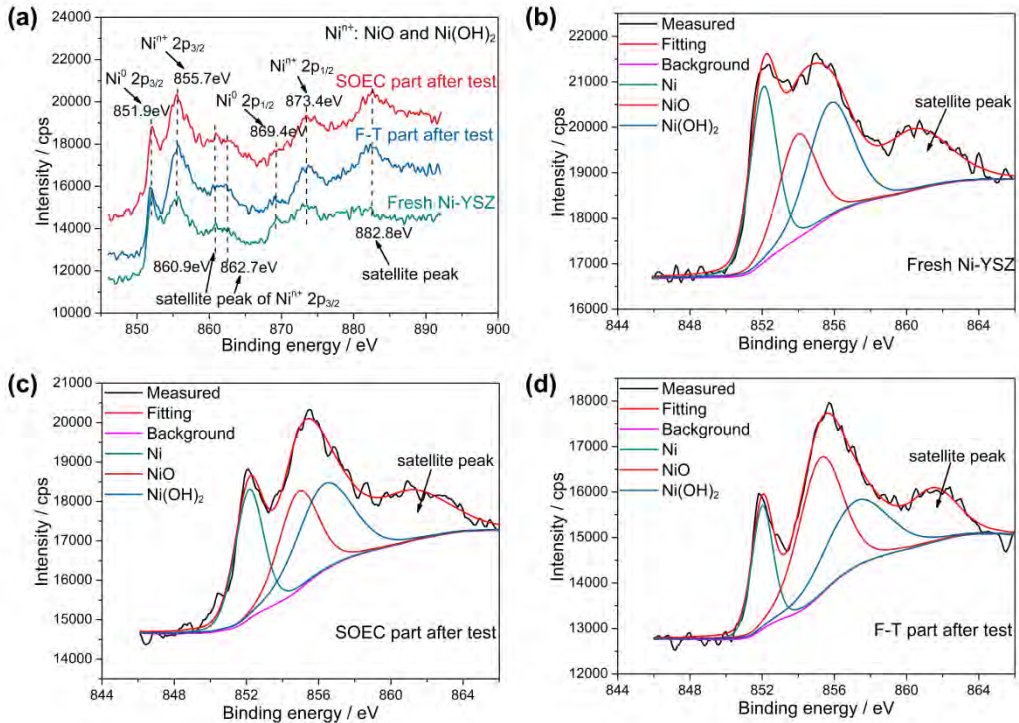


Fig. S6 XPS spectra of Ni 2p region registered for Ni-YSZ before and after 24 h test

(a). Ni 2p_{3/2} spectra from (b) fresh sample, (c) SOEC part after 24 h test and (d) F-T part after 24 h test fitted with three species: metallic Ni, NiO and Ni(OH)₂.

The chemical composition of the samples was analyzed by X-ray photoelectron spectroscopy (XPS) (Thermo Electron ESCALAB-250). All the binding energy data were calibrated by C 1s component at 284.8 eV. A basically unchanged Ni 2p XPS spectra are present after 24 h short term test (Fig. S6a). For further study the chemical state change of Ni, the Ni 2p_{3/2} peak in Fig. S6a have been fitted with three peaks. Due to the complexity of the Niⁿ⁺ species (*e.g.*, NiO, Ni(OH)₂, NiO(OH) and Ni₂O₃ etc),^{3,4} we only ascribe the Niⁿ⁺ to two most likely species, *i.e.* NiO, Ni(OH)₂ in this work. In Fig. S6b-d, a peak located at 852.1 ± 0.1 eV, which is assigned to the metallic Ni, peaks located at 854.7 ± 0.6 and 856.4 ± 0.7 eV, which can be attributed

to the NiO and Ni(OH)₂, respectively. The area ratios of three Ni species (Ni : NiO : Ni(OH)₂) are 1 : 0.83 : 1.09 for fresh Ni-YSZ, 1 : 1.05 : 1.30 and 1 : 2.32 : 1.60 for the Ni-YSZ at SOEC part and F-T part, respectively. A increased amount of Niⁿ⁺ can be the reason for the increased ohmic resistance in the Fig. S6 after 24 h test. However, the partial oxidation of Ni shows no significant depressed effect on the SOEC performance. Moreover, the methanation process produce more H₂O, thus Ni oxidation and hydroxylation is more evident at Ni-YSZ in F-T part process after 24h teat. However, the stable CH₄ yield during the 24h short-term test demonstrates the fairly stable Ni catalytic activity for the CO_x hydrogenation.

References

1. L. Chen, M. T. Yao and C. R. Xia, *Electrochem. Commun.*, 2014, **38**, 114-116.
2. C. Yang, Z. Yang, C. Jin, M. Liu and F. Chen, *Int. J. Hydrogen Energy*, 2013, **38**, 11202-11208.
3. I. Czekaj, F. Loviat, F. Raimondi, J. Wambach, S. Biollaz and A. Wokaun, *Appl. Catal. a-Gen.*, 2007, **329**, 68-78.
4. Y. H. Huang, J. J. Wang, Z. M. Liu, G. D. Lin and H. B. Zhang, *Appl. Catal. a-Gen.*, 2013, **466**, 300-306.